ACS NANO

www.acsnano.org

ARTICLE

In Situ Mechanical Testing of Nanostructured Bijel Fibers

Martin F. Haase, Nima Sharifi-Mood,[†] Daeyeon Lee,[*] and Kathleen J. Stebe[*]

Department of Chemical and Biomolecular Engineering, University of Pennsylvania, Philadelphia, Pennsylvania 19104, United States

Supporting Information

ABSTRACT: **Bijels are a class of soft materials with potential for application in diverse areas including healthcare, food, energy, and reaction engineering due to their unique structural, mechanical, and transport properties. To realize their potential, means to fabricate, characterize, and manipulate bijel mechanics are needed. We recently developed a method based on solvent transfer-induced phase separation (STRIPS) that enables continuous fabrication of hierarchically structured bijel fibers from a broad array of constituent fluids and nanoparticles using a microfluidic platform. Here, we introduce an *in situ* technique to characterize bijel fiber mechanics at initial and final stages of the formation process within a microfluidics device. By manipulation of the hydrodynamic stresses applied to the fiber, the fiber is placed under tension until it breaks into segments. Analysis of the stress field allows fracture strength to be inferred; fracture strengths can be as high as several thousand Pa, depending on nanoparticle content. These findings broaden the potential for the use of STRIPS bijels in applications with different mechanical demands. Moreover, our *in situ* mechanical characterization method could potentially enable determination of properties of other soft fibrous materials made of hydrogels, capillary suspensions, colloidal gels, or high internal phase emulsions.**

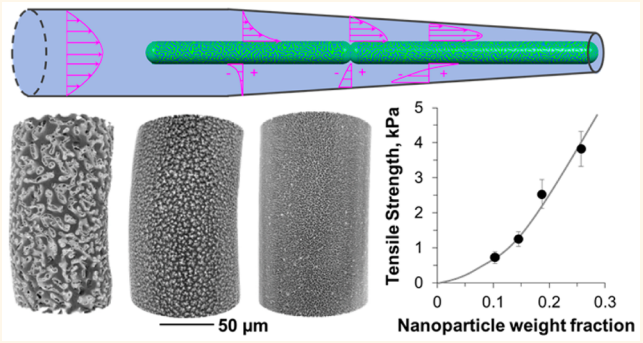

KEYWORDS: *bijels, phase separation, particle-stabilized emulsion, micromechanics, tensile testing*

Bicontinuous interfacially jammed emulsions (bijels) are a class of soft materials,[1] formed by arresting the spinodal decomposition of a mixture *via* interfacial attachment and jamming of colloidal particles.[2,3] Bijels have two interpenetrating, continuous networks of immiscible liquids, stabilized by a jammed layer of nanoparticles at their interface.[4,5] This structure has rich possibilities in application; for example, the immiscible fluids can serve as reaction or separation media, and the nanoparticles could serve as catalysts or provide other functionalities.[6,7] Moreover, by selectively polymerizing one of the bicontinuous liquids, solidified bijels can be used as sensors,[8] filtration devices, tissue engineering scaffolds,[9] and catalytic membranes.[10]

We recently reported a method to generate nanostructured bijels *via* solvent transfer-induced phase separation (STRIPS). In STRIPS, a homogeneous ternary fluid mixture of oil, water, and solvent is triggered to undergo spinodal phase separation by solvent removal. The interpenetrating network of fluids that develops during this process is arrested by the interfacial adsorption of nanoparticles suspended in the fluid mixture. This method complements the thermally induced phase separation method, which is limited to mixtures of fluids that can undergo thermal spinodal decomposition and to nanoparticles with particular wetting properties.[1,11,12] With STRIPS, bijels can be fabricated with a broad palette of immiscible liquids and surface-active nanoparticles in a continuous process. In particular, nanostructured bijel fibers can be made continuously in microfluidics devices; in these settings, solvent removal occurs by predominantly radial fluxes, generating hierarchical architectures within the fibers.

Means to characterize the mechanical properties of bijels are needed to understand how they can be tailored *via* changes in constituents or hierarchical internal structures and to lend insight into mechanisms. The rheological properties of bijels made using the conventional method, for instance, have been shown to undergo transitions like those observed in colloidal gelation to form semisolid structures, and their mechanical properties depend on the surface tension, particle interactions, and the stage of bijel maturity.[9,12−15] The mechanical properties of STRIPS bijels during their formation and their dependence on processing parameters, however, have not been investigated in detail. In this research, bijel fibers are characterized *in situ* within the microfluidics device as they are formed, facilitated by the ability to rapidly and continuously

Received: April 20, 2016
Accepted: May 26, 2016

DOI: 10.1021/acsnano.6b02660
ACS Nano XXXX, XXX, XXX−XXX

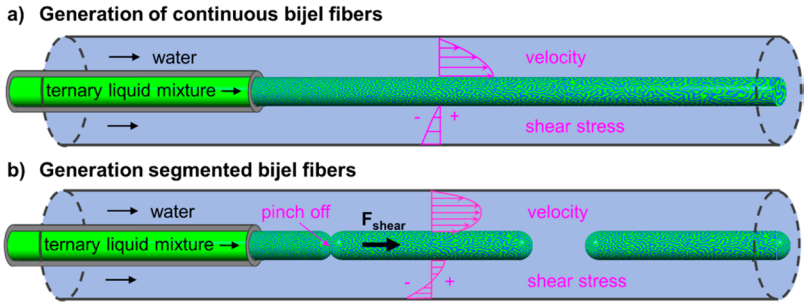

Figure 1. Controlled fiber formation. Water flows through a cylindrical channel of 300 μm diameter. A ternary liquid mixture doped with surface-active nanoparticles emerges from a central nozzle with a 50 μm diameter and evolves through a viscoelastic transition to form a bijel fiber upon phase separation and interfacial particle jamming. (a) When flow rates of inner and outer fluids are appropriately balanced, bijel fibers form continuously. (b) When the flow rate of the outer water phase is increased, associated shear stresses on the fiber cause the fiber to pinch-off periodically to form segments.

characterize a large number of samples and the exquisite control over flow fields and stresses afforded in microfluidics settings.[16] The device and flow field[17] are designed so that hydrodynamic stresses place the fibers under tension and result in the segmentation of fibers at well-defined sites within the device. Once they break off, these fiber segments are convected away, allowing for subsequent characterization of the fracture strength of bijel fibers at later stages of maturation.[18,19] The *in situ* technique allows us to probe the dependence of bijel mechanics on parameters including the volume fraction of nanoparticles and the flow rates of the fluid phases in the microfluidic device. Finally, while we focus here on nanostructured bijel fibers, in principle, other soft fibrous materials could be readily characterized in such settings to characterize their elastic modulus and fracture strength.

RESULTS AND DISCUSSION

Formation of Bijel Fibers with Controlled Length. A STRIPS bijel fiber is formed in a microfluidic device by continuously injecting a ternary liquid mixture containing suspended nanoparticles through a small glass capillary into a larger capillary that carries a water stream (Figure 1). The ternary liquid mixture contains diethyl phthalate (DEP), ethanol, and water doped with silica nanoparticles and cetyltrimethylammonium bromide (CTAB). Although this mixture has a viscosity comparable to that of water while inside the inner glass capillary, it rapidly forms a viscoelastic thread that transitions with time to form a bijel fiber upon contact with the water stream. This occurs as ethanol enters the external water stream; the loss of solvent from the ternary phase causes DEP and water to phase separate, forming fluid interfaces and interpenetrating channels.[20] Concomitantly, CTAB-modified silica nanoparticles attach to these interfaces, forming a jammed structure.[21] Long bijel fibers form continuously when the flow rate of the outer stream Q_W is sufficiently low (Figure 1a). When Q_W exceeds some threshold, however, fibers pinch-off periodically (Figure 1b) to form reproducible segments that are not yet fully matured bijels. After detachment, the segments migrate downstream and continue to evolve *via* solvent loss to form bijel fibers of finite length. Characterization of these mature bijel segments is of tremendous importance, which will be discussed in the second part of this paper.

Figure 2a shows micrographs of the fibers produced at different flow rates of the external water phase at a fixed flow rate of the ternary liquid mixture (Q_T = 50 μL/h) (see also Supporting Information video 1). For water flow rates Q_W < 1.5 mL/h, a continuous thread forms. Increasing Q_W > 2 mL/h causes the thread to pinch-off periodically into segments; the greater Q_W, the shorter the segments; for example, segments of 4 mm form at Q_W = 2.5 mL/h; segments of 1 mm form at Q_W = 4 mL/h, and very short segments, less than 0.4 mm long, form at Q_W = 13 mL/h.

As shown in Figure 2, upon exiting the formation device, the segmented and continuous fibers retain their shapes, which range from small aspect ratio (length/diameter <10) blobs to elongated rods. Associated three-dimensional confocal microscopy images reveal the internal structure of STRIPS bijels, featuring a bicontinuous oil/water architecture that can be tuned by adjusting the CTAB and silica nanoparticle concentrations (Figure 2b).[21] Figure 2c summarizes the dependence of fiber length on the ratio of Q_W and Q_T. The topmost curve in Figure 2c marks the transition between continuous fibers to rods, which flattens logarithmically with increasing ternary flow rate. Thus, for Q_T greater than 500 μL/h, fibers do not break into segments. Rather, in this regime, increasing Q_W simply decreases the diameter of the continuous fibers. For a lower Q_T, the fiber breaks into segments. Lines of constant segment length (presented in terms of segment length to diameter) are shown in this figure. These lines also follow a logarithmic trend. Segments formed for flow rates below these lines have aspect ratios smaller than the aspect ratio that corresponds to the line. The iso-aspect ratio lines pack densely close to the transition curve. Thus, fibers with high aspect ratios (>200) can only be obtained in a narrow flow rate window.

To probe this dependence, we approximate the phase-separating fibers as solid-like materials. We calculate the axial velocity profile in the external water stream $v_z(r)$ in cylindrical coordinates, where r is the radius from the axis of the channel. We also calculate the associated shear stresses and forces exerted on the fiber assuming no slip boundary conditions at the outer wall (located at $r = R_2$) and the fiber surface (located at $r = R_1$), so that $v_z|_{r=R_2} = 0$ and $v_z|_{r=R_1} = U$ (the velocity of the fiber), respectively:[22]

$$v_z(r) = -\frac{dp}{dz}\frac{(R_2^2 - r^2)}{4\mu} + \left\{U + \frac{dp}{dz}\frac{(R_2^2 - R_1^2)}{4\mu}\right\}\frac{\ln(R_2/r)}{\ln(R_2/R_1)} \quad (1)$$

DOI: 10.1021/acsnano.6b02660
ACS Nano XXXX, XXX, XXX−XXX

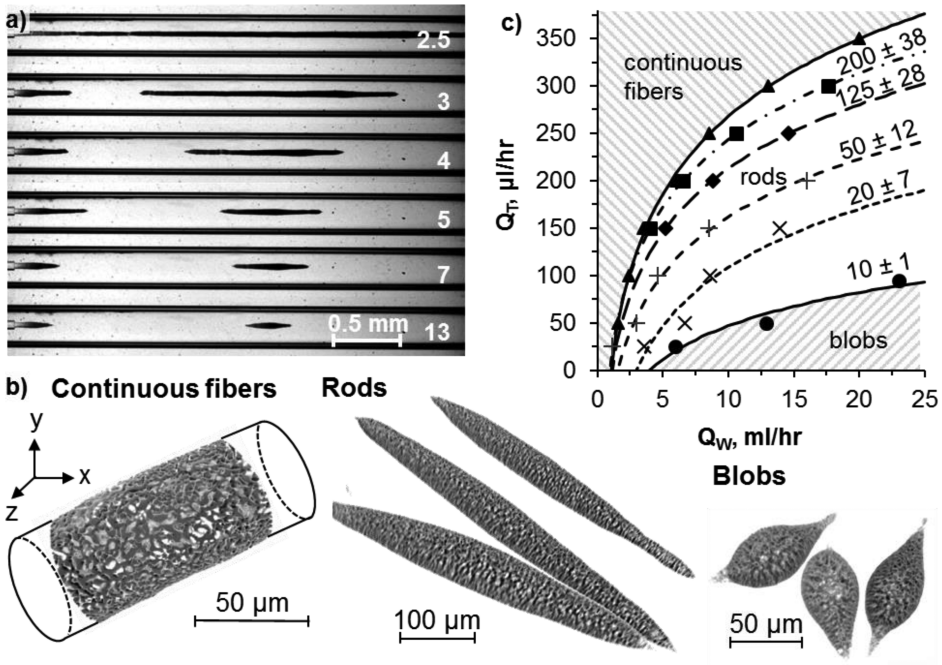

Figure 2. Tunability of fiber length and morphology. (a) Snapshots of the fiber formation in the coaxial microfluidic channel. Numbers correspond to the water flow rates in mL/h. (b) Three-dimensional confocal micrographs of continuous bijel fibers, bijel rods, and bijel blobs. Dark areas correspond to oil and bright areas to water domains. (c) Fiber length dependence on the flow rates. The curves in the diagram correspond to flow rate combinations resulting in constant fiber lengths (expressed as aspect ratio ± standard deviation). The curves are obtained by fitting the experimental data shown in Figure 3a and Figure S6. For each flow rate combination, the standard deviation of a given aspect ratio is calculated from at least 20 measurements.

$$T_{rz}|_{r=R_1} = \mu \frac{(U_0 - U)}{R_1} \frac{1}{\ln(R_2/R_1)} \tag{2}$$

where

$$U_0 = \frac{-{R_1}^2}{4\mu} \frac{dp}{dz} \left[\frac{({R_2}^2 - {R_1}^2)}{{R_1}^2} - 2\ln(R_2/R_1) \right]$$

and

$$T_{rz}|_{R_1} = \mu \left. \frac{dv_z}{dr} \right|_{R_1}$$

is the shear stress on the fiber exerted by the water phase, where dp/dz the axial pressure drop, U the fiber velocity, and μ the dynamic viscosity of the outer continuous phase. U_0 physically represents the velocity of the fiber for which zero shear force is exerted on the fiber surface. The associated shear force on the fiber of length L_c is

$$F_z|_{R_1} = T_{rz}|_{R_1} 2\pi R_1 L_c = \mu(U_0 - U) L_c \frac{2\pi}{\ln(R_2/R_1)} \tag{3}$$

A feature of this simple flow field is that the sign of the shear stress can change, as shown schematically in Figure 1. If the fiber moves slowly ($U < U_0$), the shear stress is dominated by the pressure driven flow and pulls in the $+z$ direction. If, however, the fiber moves quickly ($U > U_0$), the translating fiber dominates the flow field and the shear stress pulls in the $-z$ direction. In the bijel formation process, U is determined by the complex phenomena associated with the balance of the rates of ternary fluid injection Q_T, outer water flow rate Q_W, orifice size, as well as the rates of ethanol loss and water uptake as the fiber migrates downstream. In the experiment, we measure U by high-speed video microscopy at the last few frames before pinch-off (within 5 ms of pinch-off, with precisions of typically ±2 mm/s; see Supporting Information), and dp/dz is calculated for a given water flow rate Q_W (see Supporting Information). We find that the transition from continuous to segmented fibers occurs at low, positive shear force. Notably, as fiber segments undergo pinch-off, no measurable elastic behaviors like stretching or retraction are observed.

What determines the pinch-off length L_c? The shear force on the fiber increases linearly with the fiber length (eq 3). When the fiber has length L_c, the net force pulling downstream exceeds the fracture strength $\sigma_{c,i}$ of the fiber (subscript i denotes the initial stage of bijel formation), causing a segment of the fiber to break off. A bounding value for the length can be extracted from the balance at the cross section of the fiber where break off occurs:

$$F_z|_{R_1} = 2\pi R_1 L_c T_{rz}|_{R_1} = \pi {R_1}^2 \sigma_{c,i} \tag{4}$$

These relationships imply $L_c = \frac{R_1 \sigma_{c,i}}{2T_{rz}|_{R_1}}$. Segmented fiber lengths L_c indeed depend strongly on Q_W (Figure 3a); these data, recast based on the hydrodynamic calculations, are shown in Figure 3b, in which L_c is plotted against the inverse shear stress. The predicted linear dependence of L_c on the inverse shear stress is confirmed; the slope of this line allows $\sigma_{c,i}$ to be inferred. From this analysis, we find that $\sigma_{c,i}$ for the segments during pinch-off ranges from 90 to 300 Pa and that $\sigma_{c,i}$ increases with Q_T.

To understand the physical reason behind this trend, we analyze the pinch-off event at different Q_T values by carefully monitoring the relative grayscales of the fibers (ratio of the grayscale at some distance from the nozzle to that when bijel formation is complete (4 cm from the nozzle)) in the regions

DOI: 10.1021/acsnano.6b02660
ACS Nano XXXX, XXX, XXX−XXX

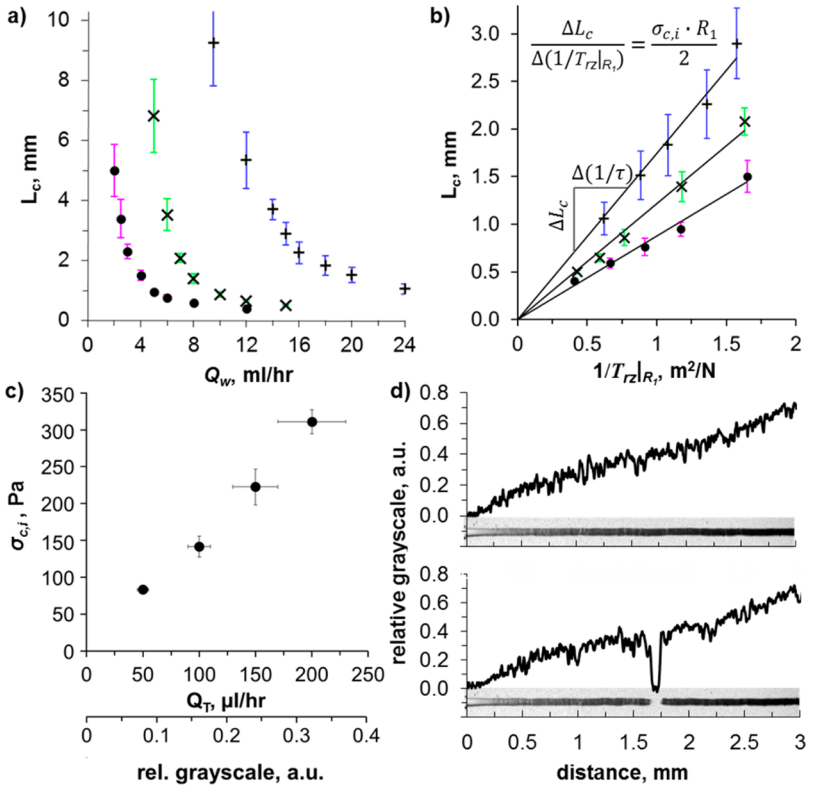

Figure 3. Analysis of bijel fiber segmentation. (a) Fiber length L_c plotted against water flow rate Q_W for different ternary flow rates Q_T: (●) 50 µL/h, (×) 100 µL/h, (+) 200 µL/h. Vertical error bars: standard deviation of fiber length. (b) Fiber length plotted against the inverse shear stress. Because of the increasing error of $1/T_{rz}|_{R_1}$ and the larger standard deviation of L_c at low $T_{rz}|_{R_1}$, we consider only data points for $T_{rz}|_{R_1}$ > 0.6 N/m² for determining the linear trend. (c) Fracture strength $\sigma_{c,i}$ of the fiber plotted against Q_T and the relative grayscale (lower *x*-axis). Horizontal error bars are the standard deviation of relative grayscale. (d) Relative grayscale, defined as the gray value of the fiber divided by the final gray value plotted against the distance from the fiber nozzle. Silica weight fraction for all experiments is 0.197 g_{silica}/g_{total}, and CTAB concentration is 40 mM with respect to the total volume of the initial ternary mixture.

around the pinch-off. The relative grayscale increases as bijel matures owing to phase separation and interfacial particle jamming. Prior to pinch-off (Figure 3d, top), the relative grayscale increases more or less linearly with the distance from the nozzle. Upon pinch-off, the grayscale profile shows an abrupt dip due to the appearance of the bright background. We find that the relative grayscale measured at the ruptured ends increases with Q_T (see lower *x*-axis in Figure 3c and Supporting Information) and that the pinch-off occurs further downstream as Q_T is increased. Based on the location of pinch-off and the velocity of the fiber (U), we infer that the residence time for the region of the fiber that undergoes pinch-off also increases with Q_T (see Supporting Information). Moreover, we observe thinning of the viscoelastic thread as Q_T is increased, which would facilitate radial mass transfer of ethanol and thus lead to higher extent of phase separation, again consistent with the increased $\sigma_{c,i}$ with Q_T (see Supporting Information). All of these observations indicate the region of the fiber that undergoes pinch-off undergoes a greater extent of phase separation with increasing Q_T, consistent with the trend seen in Figure 3c.

This analysis of the pinch-off phenomenon allows us to probe $\sigma_{c,i}$ in the early stages of bijel formation. However, pinch-off in the uniform cross section channel always occurs before the formation process is complete (Figure 2b). The tensile strength of the final material ($\sigma_{c,f}$) is a parameter of utmost relevance for subsequent applications of STRIPS bijel fibers. Fortunately, with small changes in device geometry, we can design flow fields to cleave mature bijel fibers.

Fracture Strengths of Mature Bijel Fibers. To characterize the tensile strength of mature bijel fibers, we apply tensile stress on fiber segments by flowing them through a conical constriction (Figure 4) far downstream from the nozzle (~5 cm from the device entrance). At this point, the grayscale profile (*i.e.*, opacity) of the fiber no longer changes, indicating the completion of bijel formation.

Remarkably, as a fiber segment flows through the constriction, it breaks into two shorter pieces. This process does not always occur at the same location and strongly depends on the total length of the fiber segment and its position in the constriction (see Supporting Information video 2); no elastic stretching or retraction is observed during these snapping events.

As a fiber segment, transported by the outer water stream, enters the constriction, both water and segment velocities increase (see Figure 4a), attaining maximum values at the narrowest point. At some critical location along the segment length, a piece breaks off and convects away. When this occurs, the remaining portion of the segment slows abruptly (see Figure 4a). This remaining portion can undergo a second breaking event as it accelerates again into the constriction.

The associated flow field is calculated within the lubrication approximation, based on the small slope in the conical region (see Supporting Information).[23] The main outcome of this analysis is that eqs 1−3 are modified to leading order, with R_2 =

DOI: 10.1021/acsnano.6b02660
ACS Nano XXXX, XXX, XXX−XXX

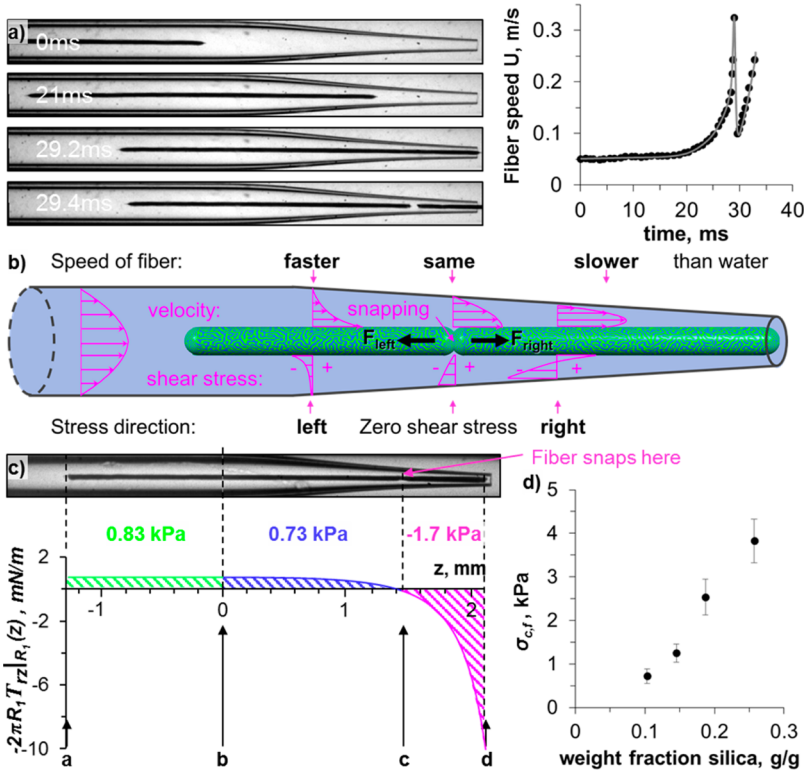

Figure 4. Measurement of the tensile strength of mature bijel fibers. Fiber characterization: After translating at constant speed through a channel of 5 cm length, a bijel fiber segment enters a conical constriction (2200 μm in length; diameters of inlet and outlet are 300 and 80 μm, respectively) under conditions of constant Q_W. In the vicinity of the constriction, the water stream velocity increases and associated shear forces locally accelerate and strain the semisolid fiber, causing it to be torn apart in the channel. Analysis of this event allows the fiber tensile strength to be determined. (a) Left: micrograph time series of a fiber segment entering a conical constriction. Right: velocity of the fiber over time measured by high-speed video microscopy. (b) Schematic representation of the water velocity and shear stress around the fiber. (c) Perimeter-specific shear force profile on the fiber segment over the fiber length instantaneously before pinch-off (corresponding to above micrograph, U = 190 μm/ms, Q_W = 7 mL/h, R_1 = 19 μm, $R_{2(0)}$ = 150 μm, β = 0.0486, L_{ab} = 1280 μm, L_{bc} = 1490 μm, L_{cd} = 700 μm, fiber with silica weight fraction of 0.26 g/g). Calculated shear stresses in kPa for different fiber sections obtained by integration above curve in the diagram. (d) Measured tensile strengths $\sigma_{c,f}$ of bijel fibers with different silica nanoparticle fractions.

$R_{2(0)} - \beta z$, where $R_{2(0)}$ denotes the radius of the cylindrical capillary and β denotes the slope of the taper, and, as a result, $U_0(z)$ can be derived (see Supporting Information). Calculation of the associated stresses $T_{rz}|_{R_1}$ along the fiber segment reveals the source of tension that drives segment cleavage.

At the trailing end of the fiber, $U > U_0(z)$, thus shear pulls in the $-z$ direction, while at the leading end, $U < U_0(z)$, so shear pulls in the $+z$ direction. The fiber breaks near the location where the shear stress changes sign, labeled c in Figure 4c, to form a segment of length determined by the fracture strength. The shear force in the $-z$ direction, $F_{\text{left}} = 2\pi(\int_a^b R_1(z)T_{rz}|_{R_1}\mathrm{d}z + \int_b^c R_1(z)T_{rz}|_{R_1}\mathrm{d}z)$, includes contributions from the shear force on the fiber in the cylindrical region and at the entrance to the conical regions, whereas the shear force in the $+z$ direction, $F_{\text{right}} = 2\pi L(\int_c^d R_1(z)T_{rz}|_{R_1}\mathrm{d}z)$ (where d denotes the location of the fiber's leading end) depends on the shear force in the rest of the conical region. The longer the fiber segment between c and d, the greater the tension in the fiber at point c. Snap-off occurs when the opposing shear forces exceed the fiber tensile strength:

$$\pi R_1(z=c)^2\sigma_{c,f} = 2\pi(\int_a^b R_1(z)T_{rz}|_{R_1}\mathrm{d}z + \int_b^c R_1(z)T_{rz}|_{R_1}\mathrm{d}z) - 2\pi(\int_c^d R_1(z)T_{rz}|_{R_1}\mathrm{d}z) \quad (5)$$

From this balance, we infer $\sigma_{c,f}$. The tensile strength depends strongly on the weight percent of silica nanoparticles in the original ternary mixture, ranging from a few hundred Pa at 10 wt % silica particles up to 4000 Pa (comparable to calcium cross-linked alginate hydrogel)[24] at 25 wt % silica particles (Figure 4c). We attribute this increase to the increased number of coagulated silica particles, most likely adhering to each other *via* various attractive interactions such as van der Waals, hydrophobic interactions, and capillary forces.[14] We find that $\sigma_{c,f}$ is only weakly dependent on CTAB concentration, in spite of the critical role the surfactant plays in altering the internal architecture of the fibers (see Supporting Information). These differences might affect other mechanical properties of the fibers, such as the bending modulus, as indicated by our observation that fibers prepared with higher CTAB concentrations have lower tendency to kink under their own weight when exiting the glass capillary channel into a vial filled with stagnant water.

DOI: 10.1021/acsnano.6b02660
ACS Nano XXXX, XXX, XXX−XXX

CONCLUSIONS

Bijels are an emerging class of soft materials with promising applications in food science, reaction engineering, and membrane separation due to their unique structural, mechanical, and transport properties. Here, we introduce a microfluidic technique to form nanostructured STRIPS bijel fibers of controlled aspect ratio and to measure their mechanical strength in the initial stages of bijel formation. Moreover, using a tapered geometry, we apply tensile stress on bijel fiber segments to measure the fracture strength of mature STRIPS bijels. Using this method, we find that the tensile strength of the bijel fibers depends strongly on the nanoparticle concentration and can be tuned over 2 orders of magnitude. In future experiments, this microfluidic method will be used for the mechanical characterization of bijels made with different building blocks as well as the assessment of bijel postprocessing such as interfacial particle cross-linking. Moreover, this technique, we believe, is not limited to the characterization of bijels and has broad potential for the *in situ* mechanical characterization of other soft fibers, composed of hydrogels,[25] colloidal gels, high-internal phase emulsions,[26] or capillary suspensions.[27]

EXPERIMENTAL SECTION

Materials. Twenty-two nanometer SiO_2 nanoparticles (Ludox TMA), CTAB (BioUltra >99%), and diethyl phthalate (99.5%) were purchased from Sigma-Aldrich and used as received. Pure water and pure ethanol (200 proof, >99.5%) were used for all experiments.

Preparation of Suspensions/Solutions. The ternary liquid mixture comprises five main components: (i) pure ethanol, (ii) a solution of 200 mM CTAB in ethanol, (iii) a suspension of 22 nm SiO_2 silica nanoparticles in water at pH 3, (iv) pure water, and (v) DEP. The original SiO_2 suspension has a silica concentration of 44.2 wt % and a pH value between 5 and 7. We titrated this suspension to pH 3 by adding 1 M hydrochloric acid dropwise. As an example, we describe the preparation of a 5 mL solution for the generation of a bijel fiber with 25 mM CTAB and 10.4 wt % silica particles in a ternary mixture composed of 40.8 vol % DEP, 40.8 vol % ethanol, and 18.4 vol % water. This mixture corresponds to 2.04 mL of DEP, 1.43 mL of pure ethanol, 0.6 mL of the 200 mM CTAB in ethanol solution, and 0.92 mL of the 44.2 wt % Ludox TMA suspension. Simply shaking a mixture containing all the components is enough to produce a clear homogeneous solution with well-dispersed silica nanoparticles. To increase the silica concentration further, the suspension was heated to 130 °C under a nitrogen stream to evaporate the ethanol and water. After the evaporation, we add 0.92 mL of the 44.2 wt % silica suspension and 2.04 mL of pure ethanol to obtain a dispersion with 18.8 wt % silica particles.

Microfluidic System. To produce STRIPS bijels and characterize their mechanical properties, we use a glass-capillary-based microfluidic device consisting of two concentric cylindrical glass capillaries glued onto a microscope slide. A round capillary with 80 μm outer diameter was centered in a round capillary with 300 μm inner diameter. Both capillaries were connected through dispensing needles to two separate syringe pumps. Into the larger capillary we pumped an aqueous solution with a pH value of 3 and 1 mM CTAB at laminar conditions (Re < 50). Through the 50 μm orifice of the smaller capillary, a ternary liquid mixture containing silica nanoparticles and CTAB was introduced. For the measurement of the final bijel fracture strength, the outer round capillary (300 μm) was tapered with a micropipette puller (Sutter P-97) at a distance 5 cm from the injection nozzle. For all experiments, the centered alignment of the injection nozzle was crucial.

Microscopy. An inverted light microscope (Nikon Diaphot 300) equipped with a high-speed camera (Phantom V7) was used to visualize the fiber formation and rupture at a frame rate of 500−8000 Hz. To visualize the three-dimensional structure of the bijel fibers, we added Nile red to the ternary mixture and collected fibers on a microscope slide. With a confocal microscope, we acquired confocal *z*-stacks and reconstructed the three-dimensional structure with the software ImageJ.

ASSOCIATED CONTENT

Supporting Information

The Supporting Information is available free of charge on the ACS Publications website at DOI: 10.1021/acsnano.6b02660.

Calculations on lubrication approximation validation, velocity and shear stress profiles, fiber velocity measurements during pinch-off, fracture strength dependence on Q_T and the concentration of CTAB (PDF)
Video 1 (AVI)
Video 2 (AVI)

AUTHOR INFORMATION

Corresponding Authors

*E-mail: daeyeon@seas.upenn.edu.
*E-mail: kstebe@seas.upenn.edu.

Present Address

†(N.S.-M.) CD-adapco, A Siemens Business, Lebanon, New Hampshire 03766, United States

Notes

The authors declare no competing financial interest.

ACKNOWLEDGMENTS

We thank Prof. Randall Kamien for helpful discussions, and Prof. Ivan J. Dmochowski for generously providing access to the confocal laser scanning microscope. This work is supported by NSF CBET-1449337 and Penn MRSEC DMR11-20901 through the NSF. M.F.H. is supported by the German Research foundation (DFG) under the project number HA 7488/1-1.

REFERENCES

(1) Herzig, E. M.; White, K. A.; Schofield, A. B.; Poon, W. C. K.; Clegg, P. S. Bicontinuous Emulsions Stabilized Solely by Colloidal Particles. *Nat. Mater.* **2007**, *6*, 966−971.

(2) Bray, A. J. Theory of Phase-Ordering Kinetics. *Adv. Phys.* **1994**, *43*, 357−459.

(3) Stratford, K.; Adhikari, R.; Pagonabarraga, I.; Desplat, J.-C.; Cates, M. E. Colloidal Jamming at Interfaces: A Route to Fluid-Bicontinuous Gels. *Science* **2005**, *309*, 2198−2201.

(4) Cates, M. E.; Clegg, P. S. Bijels: A New Class of Soft Materials. *Soft Matter* **2008**, *4*, 2132−2138.

(5) Tavacoli, J. W.; Thijssen, J. H. J.; Clegg, P. S. Bicontinuous Emulsions Stabilized by Colloidal Particles. In *Particle-Stabilized Emulsions and Colloids*; Bon, S., Ngai, T., Eds.; Royal Society of Chemistry: Cambridge, U.K., 2015; p 129.

(6) Crossley, S.; Faria, J.; Shen, M.; Resasco, D. E. Solid Nanoparticles that Catalyze Biofuel Upgrade Reactions at the Water/Oil Interface. *Science* **2010**, *327*, 68−72.

(7) Pera-Titus, M.; Leclercq, L.; Clacens, J. M.; De Campo, F.; Nardello-Rataj, V. Pickering Interfacial Catalysis for Biphasic Systems: From Emulsion Design to Green Reactions. *Angew. Chem., Int. Ed.* **2015**, *54*, 2006−2021.

(8) Lee, M. N.; Mohraz, A. Bicontinuous Macroporous Materials from Bijel Templates. *Adv. Mater.* **2010**, *22*, 4836−4841.

(9) Witt, J. A.; Mumm, D. R.; Mohraz, A. Bijel Reinforcement by Droplet Bridging: A Route to Bicontinuous Materials with Large Domains. *Soft Matter* **2013**, *9*, 6773−6780.

(10) Lee, M. N.; Mohraz, A. Hierarchically Porous Silver Monoliths from Colloidal Bicontinuous Interfacially Jammed Emulsion Gels. *J. Am. Chem. Soc.* **2011**, *133*, 6945−6947.

DOI: 10.1021/acsnano.6b02660
ACS Nano XXXX, XXX, XXX−XXX

(11) Tavacoli, J. W.; Thijssen, J. H. J.; Schofield, A. B.; Clegg, P. S. Novel, Robust, and Versatile Bijels of Nitromethane, Ethanediol, and Colloidal Silica: Capsules, Sub-Ten-Micrometer Domains and Mechanical Properties. *Adv. Funct. Mater.* **2011**, *21*, 2020−2027.
(12) Bai, L.; Fruehwirth, J. W.; Cheng, X.; Macosko, C. W. Dynamics and Rheology of Nonpolar Bijels. *Soft Matter* **2015**, *11*, 5282−5293.
(13) Lee, M. N.; Thijssen, J. H. J.; Witt, J. A.; Clegg, P. S.; Mohraz, A. Making a Robust Interfacial Scaffold: Bijel Rheology and its Link to Processability. *Adv. Funct. Mater.* **2013**, *23*, 417−423.
(14) Sanz, E.; White, K. A.; Clegg, P. S.; Cates, M. E. Colloidal Gels Assembled via a Temporary Interfacial Scaffold. *Phys. Rev. Lett.* **2009**, *103*, 255502.
(15) Reeves, M.; Brown, A. T.; Schofield, A. B.; Cates, M. E.; Thijssen, J.H.J. Particle-Size Effects in the Formation of Bicontinuous Pickering Emulsions. *Phys. Rev. E* **2015**, *92*, 032308.
(16) Dudani, J. S.; Gossett, D. R.; Tse, H. T. K.; Di Carlo, D. Pinched-Flow Hydrodynamic Stretching of Single-Cells. *Lab Chip* **2013**, *13*, 3728−3734.
(17) Attia, R.; Pregibon, D. C.; Doyle, P. S.; Viovy, J. L.; Bartolo, D. Soft Microflow Sensors. *Lab Chip* **2009**, *9*, 1213−1218.
(18) Wyss, H. M.; Franke, T.; Mele, E.; Weitz, D. A. Capillary micromechanics: Measuring the Elasticity of Microscopic Soft Objects. *Soft Matter* **2010**, *6*, 4550−4555.
(19) Duprat, C.; Berthet, H.; Wexler, J. S.; du Roure, O.; Lindner, A. Microfluidic in Situ Mechanical Testing of Photopolymerized Gels. *Lab Chip* **2015**, *15*, 244−252.
(20) Haase, M. F.; Brujic, J. Tailoring of High-Order Multiple Emulsions by the Liquid−Liquid Phase Separation of Ternary Mixtures. *Angew. Chem.* **2014**, *126*, 11987−11991.
(21) Haase, M. F.; Stebe, K. J.; Lee, D. Continuous Fabrication of Hierarchical and Asymmetric Bijel Microparticles, Fibers, and Membranes by Solvent Transfer-Induced Phase Separation (STRIPS). *Adv. Mater.* **2015**, *27*, 7065−7071.
(22) Bird, R. B. *Transport Phenomena*; Wiley: New York, 1960; pp 51−54.
(23) Deen, W. M. *Analysis of Transport Phenomena, Topics in Chemical Engineering*; Oxford University Press: New York, 1998.
(24) Sun, J. Y.; Zhao, X.; Illeperuma, W. R.; Chaudhuri, O.; Oh, K. H.; Mooney, D. J.; Vlassak, J. J.; Suo, Z. Highly Stretchable and Tough Hydrogels. *Nature* **2012**, *489*, 133−136.
(25) Daniele, M. A.; North, S. H.; Naciri, J.; Howell, P. B.; Foulger, S. H.; Ligler, F. S.; Adams, A. A. Rapid and Continuous Hydrodynamically Controlled Fabrication of Biohybrid Microfibers. 6. *Adv. Funct. Mater.* **2013**, *23*, 698−704.
(26) Bell, R. V.; Parkins, C. C.; Young, R. A.; Preuss, C. M.; Stevens, M. M.; Bon, S. A. F. Assembly of Emulsion Droplets into Fibers by Microfluidic Wet Spinning. *J. Mater. Chem. A* **2016**, *4*, 813−818.
(27) Koos, E. Capillary suspensions: Particle Networks Formed Through the Capillary Force. *Curr. Opin. Colloid Interface Sci.* **2014**, *19*, 575−584.

DOI: 10.1021/acsnano.6b02660
ACS Nano XXXX, XXX, XXX−XXX